Imaging of DNA hybridization on microscopic polypyrrole patterns using scanning electrochemical microscopy (SECM): the HRP bio-catalyzed oxidation of 4-chloro-1-naphthol

Elodie Fortin,[b] Pascale Mailley,[b] Loic Lacroix[a] and Sabine Szunerits*[a]

We illustrate in this paper the successful combination of the direct and feedback mode of scanning electrochemical microscopy (SECM) for the writing of oligonucleotide patterns on thin gold films alongside the imaging of DNA hybridization. The patterning process was achieved using the direct mode of SECM, where the electrical field established between the SECM tip and the gold interface was used to drive the local deposition of micrometre sized polypyrrole spots to which a 15^{mer} oligonucleotide (ODN) strand was linked covalently. Imaging of the deposited polypyrrole-ODNs was achieved by means of the feedback mode of SECM using $Ru(NH_3)_6^{3+}$ as the mediator. The detection of the hybridization reaction of the ODN probes with their biotinylated complementary strands using SECM was possible after subsequent reactions with streptavidin and biotinylated horseradish peroxidase (HRP). The HRP-biocatalyzed oxidation of 4-chloro-1-naphthol (**1**) in the presence of H_2O_2, and the precipitation of the insoluble product 4-chloro-1-naphthon (**2**) on the hybridized areas on the gold film caused a local alteration of conductivity. Such a change in conductivity was sensitively detected by the SECM tip and allowed imaging of DNA arrays in a fast and straightforward way.

1. Introduction

The localized immobilization of micro to nanometre sized biological recognition elements is currently an active field of research, in particular due to an increasing demand for miniaturized bioanalytical devices together with the call for parallel analysis of multiple analytes in small sample volumes. Surface probe microscopy (SPM) techniques have attracted much attention for the site directed structuring of surfaces due to their simplicity and they are increasingly used next to lithographic approaches such as microcontact printing[1] or site selective supply of biomolecules by microfluidic networks.[2] Scanning electrochemical microscopy (SECM), a method introduced in 1989 by Bard, has been used extensively for the local deposition of biomolecules.[3–13] SECM is a non-contact scanning probe technique that uses a microelectrode for the imaging of surfaces and surface reactions. The phenomenon exploited to obtain topographic images of the target surface is that in close proximity of the microelectrode to the target surface the steady state current of the microelectrode (the tip) in the solution of a redox species (mediator) changes in a distinctive way. If the target is electrically conducting, an amplification of the steady state current is observed due to the redox recycling of the mediator by the target (positive feedback), while a non conductive interface hinders the back diffusion of the mediator to the tip causing a decrease of the current as the tip approaches the surface of the target (negative feedback). SECM has been widely used for the local modification of diverse target surfaces like the electrochemical desorption of alkanethiolates with further chemical modification,[14,15] the local deposition of gold and further functionalization by thiolates,[16] as well as the localized electropolymerization of conducting polymers.[17–20] Scanning electrochemical microscopy is however more than just a tool for the reproducible and accurate immobilization of biomolecules. One of the main advantages of using SECM is the possibility to map the surface reactivity allowing the assessment of surface reaction kinetics as well as identifying the bioactive sites. SECM has been therefore used to monitor targets of biological origin including enzymes,[6,10–13] antibodies[21,22] and cells.[23] In recent years SECM has been further used for the imaging of confined DNA molecules and DNA hybridization reactions in a highly localized surface area.[4,7–9,24] Thus far, the standard method for the detection of hybridization is confocal fluorescence imaging using fluorescence-labeled target DNA. One of the major drawbacks of fluorescence detection, besides size and price, is the quenching of the fluorescent dyes with time. Electrochemical hybridization methods are an interesting alternative to optical readouts and have been demonstrated as being sensitive and selective means for studies of DNA oxidative damage, for trace DNA analysis as well as for the detection of hybridization events.[25,26] SECM is another and different electrochemical approach to detecting surface activity changes. The use of SECM for imaging hybridization reactions is interesting as this electrochemical scanning probe method is

[a]*Laboratoire d'Electrochimie et de Physicochimie des Matériaux et des Interfaces (LEPMI), CNRS-INPG-UJF, 1130 rue de la piscine, BP 75, 38402 St. Martin d'Hères Cedex, France.*
E-mail: sabine.szunerits@lepmi.inpg.fr; Fax: +33 4 76 82 66 87; Tel: +33 4 76 82 65 52
[b]*Groupe CREAG, UMR CNRS/CEA/UJF 5819, DRFMC/SI3M, CEA, 17 rue des Martyrs, 38054 Grenoble Cedex 9, France*

comparatively inexpensive, compact and sensitive to changes in surface conductivity. Additionally, the lateral resolution of the SECM is sufficient for imaging even DNA arrays of high density. Takenaka and coworkers[24] used an electroactive hybridization indicator for the visualization of DNA microarrays with the aid of SECM. Preliminary studies for detecting DNA hybridization using glucose oxidase was reported by Toth and coworkers.[4] The imaging of surface confined DNA molecules and hybridization through guanine oxidation induced by the tip generated $Ru(bpy)^{3+}$, as well as the utilization of SECM to image DNA hybridization with silver enhancement at a DNA microarray has been shown by Wang and Zhou[9] and Zhou *et al.*[13] Schuhmann and coworkers reported recently an electrochemical detection scheme that was suited for imaging microscopic spots of immobilized nucleic acids.[7] The method is based on a modulation of diffusional mass transport of a negatively charged redox mediator (*e.g.* $[Fe(CN)_6]^{3-/4-}$) that experiences electrostatic repelling forces from deprotonated, and thus identically charged, phosphate groups of surface-anchored capture probes.

In this paper we want to give a complete portrait of the advantages and use of SECM in the field of DNA microarrays. The potential of SECM for forming DNA microspot arrays together with sensitive detection of hybridization events at these DNA microarrays will be shown. SECM will be, in other words, used for the structuring of interfaces with DNA probes as well as for the topographic and chemical imaging of the surface. One strategy for the linking of DNA to surfaces was developed by Livache and coworkers[17,20,27–33] and is based on the electropolymerization of a conducting polymer bearing an oligonucleotide unit. The polymer chosen in this paper is polypyrrole, as it has emerged as a promising material in the development of electrochemical sensors and DNA arrays due to its electronic conductivity, environmental stability, biocompatibility and easy and controlled processing by electropolymerization.[34–38] It has been recently reported by us that patterning of thin gold films with polypyrrole-oligonucleotide probes using SECM and the formation of oligonucleotide gradients on the surface is possible by localized electropolymerization.[17,20] The formation of the local polypyrrole-ODN spots is based on the generation of a potential drop between a macroscopic working electrode (the gold film) and a microscopic counter electrode (the microelectrode), a process described before by Kranz *et al.*[18,19] We discuss in this paper moreover a novel and easy hybridization detection scheme (Fig. 1C) based on the sensitive detection of conductivity change by the SECM tip. Hybridization of confined polypyrrole-ODNs with biotinylated complementary strands and subsequent reactions with streptavidin and biotinylated horseradish peroxidase (HRP) forms a molecular sandwich. The assembly linked HRP will stimulate the oxidation of 4-chloro-1-naphthol (**1**) to 4-chloro-1-naphthon (**2**) (Fig. 1B), and the precipitation of the insoluble product (**2**) on the hybridized areas on the gold film will cause a local alteration of the conductivity.[39] We show that such a change in conductivity can be sensitively detected by the SECM tip allowing imaging of DNA arrays in a fast and straightforward way.

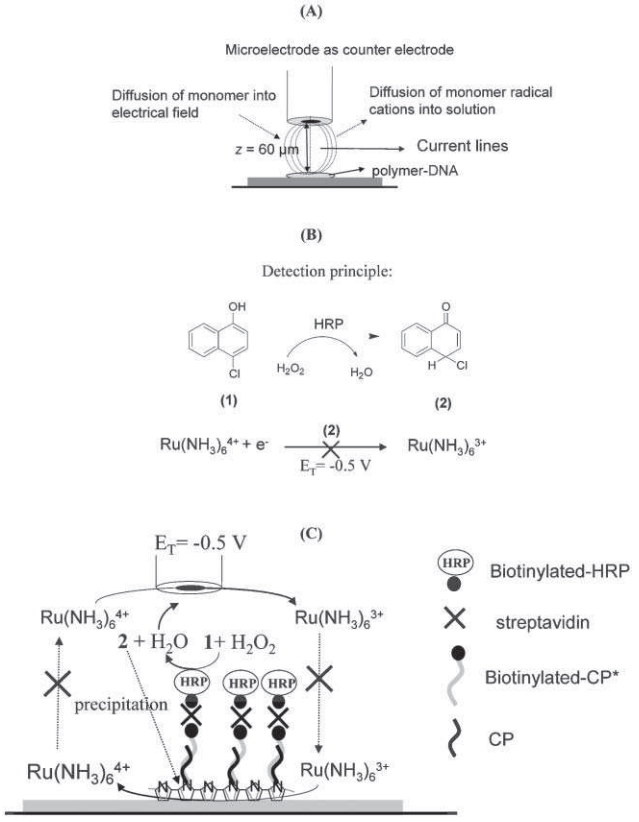

Fig. 1 (A) Schematic representation of the direct mode of SECM for the localised electropolymerization of pyrrole-ODN probes. (B) Schematic of the assembly process. (C) "Molecular Assembly" process.

2. Experimental

2.1. Materials

Hexaaminеruthenium(III) chloride ($[Ru(NH_3)_6]Cl_3$), potassium chloride (KCl), lithium perchlorate ($LiClO_4$), hydrogen peroxide (H_2O_2) and 4-chloro-1-naphthol (**1**) were purchased from Aldrich. Phosphate Buffer Saline (PBS, pH 7.4) tablets, Bovine Serum Albumin (BSA), streptavidin, and peroxidase-biotinamidocaproyl conjugate were provided by Sigma. Pt wire (diameter = 10 µm) was obtained from Goodfellow. Glass tubes were obtained from Narigishe.

Stock solutions of pyrrole (1M) were prepared from pyrrole (Acros) dissolved in HPLC grade acetonitrile (SDS) and were kept at −20 °C. Oligonucleotides (ODN) were provided by BioMérieux (formerly Apibio, CEA Grenoble, France). The pyrrole-ODNs used in this work were 5′-pyrrole-$(T)_{10}$-ACG-CCA-GCA-GCT-CCA-3′ (pyrrole-CP) with its complementary biotinylated ODN being 5′-biotin-TGG-AGC-TGC-TGG-CGT-3′ (biotin-CP*) and 5′-pyrrole-$(T)_{10}$-TGG-AGC-TGC-TGG-CGT-3′ (pyrrole-M5) with its complementary biotinylated ODN being 5′-biotin-ACG-CCA-GCA-GCT-CCA-3′ (biotin-M5*).

2.2. Preparation of the gold slides

Substrate electrodes were prepared at the platform PROMESS at the CEA Grenoble, by vacuum deposition of 5 nm of titanium and 50 nm of gold onto cleaned glass slides

(76 × 26 × 1 mm, $n = 1.58$ at $\lambda = 633$ nm, CML, France). Electrical contacts to the copper SECM support were made by using a conducting silver foil around the glass slides.

2.3. SECM set up

The SECM apparatus was built at the LEPMI in collaboration with Prof. Heinze, and is nearly identical to the one described in ref. 40. The electrodes were fabricated by first pulling a glass capillary (borosilicate, Blaubrand) with a micropipette puller (Sutter Instruments P97, Novato, CA, USA) sealing the Pt wire into the glass and polishing the surface with a Micropipette Grinder EG-44 (Narishige, Japan). In the present work a platinum microelectrode tip (diameter 10 μm, $R_g = 25$) was used to probe locally the electrochemical reactivity of the diamond surface. The approach of the microelectrode to the substrate is performed using a HEKA PG 340 ring-disk potentiostat (Lambrecht, Germany).

2.4. SPR instrumentation

The Surface Plasmon Resonance instrument used was a double-channel Autolab ESPRIT instrument (Eco Chemie, Utrecht, The Netherlands) allowing simultaneous electrochemical and SPR measurements. The configuration of this equipment is described elsewhere.[41,42] In short, polarized laser light ($\lambda = 670$ nm) is directed to the bottom side of the sensor disk *via* a hemispheric lens and the reflected light is detected using a photodiode. The angle of incidence is varied using a vibrating mirror with a frequency of 44 Hz. SPR curves were scanned on the forward and backward movement of the mirror and the minima in reflectance determined and averaged. The instrument is equipped with a cuvette of about 100 μL. The prism used was N-BAF-3 having a refractive index of $n = 1.58$.

2.5. Fluorescence imaging of the ODN spots

Quality control of the ODN spots was carried out with biotinylated complementary probes according to the procedure previously described.[17] Briefly, after washing in PBS the gold slide was incubated for 20 min in a solution of 5% streptavidin-*R*-phycoerythrin diluted in PBS. Fluorescence ($\lambda_{ex} = 550$ nm, $\lambda_{em} = 590$ nm) was recorded with an epifluorescence microscope (BX 60, Olympus) equipped with a Peltier cooled CCD camera (Hamamatsu) and imaging software (Imagepro plus, Media Cyberbetics). The regeneration step was performed by rinsing the gold surface with 200 mM NaOH to open the double helix.

2.6. Patterning of polypyrrole-oligonucleotide spots

For the copolymerization of pyrrole/pyrrole-ODN, solutions of 200 mM pyrrole/10 μM pyrrole-ODN in $LiClO_4$ (0.1M in water) were used. The potential applied was $E_{app} = 0.7$ V *vs.* Ag/AgCl and the polymerization time was $\tau = 20$ ms. The distance between the substrate (gold) and the microelectrode used here as the counter electrode was $z = 60$ μm. Approach curves for the positioning of the microelectrode to the gold substrate were carried out in an aqueous solution of 10 mM $Ru(NH_3)_6^{3+}$–0.1 M KCl using the positive feedback mode of the SECM. The tip was poised at a potential of $E_{app} = -0.5$ V *vs.* Ag/AgCl where the reduction of the $Ru(NH_3)_6^{3+}$ is diffusion controlled. The substrate was poised at $E_{app} = 0.0$ V *vs.* Ag/AgCl. By recording the tip current while approaching the gold substrate at a scan rate of 1 μm s^{-1}, the distance between the two electrodes can be determined precisely.

2.7. Construction of biological assembly for the detection of hybridization

4-Chloro-1-naphthol (**1**) (Fig. 1B) was dissolved initially in ethanol and this stock solution was diluted in PBS, to yield the developing solution that consists of **1** (10^{-3} M) and ethanol (2% v/v). Before hybridization, the gold surface was incubated for 10 min in PBS containing BSA (1%) to minimize non-complementary interactions with the gold surface. Hybridization was carried out at room temperature for 20 min in biotinylated complementary ODN (1 μM) in BSA–PBS (1%). After washing in PBS, the modified gold slide was incubated for 10 min in BSA–PBS (1%) and then for 15 min in a solution of streptavidin (0.5 mg mL^{-1}) diluted in PBS. After washing, the gold substrate was incubated in peroxidase–biotinamidocaproyl conjugate (120 U mL^{-1} in PBS) for 15 min. It was important to wash the gold slides several times with PBS to remove any traces of non-immobilized peroxidase. After that, the molecular sandwich was incubated for 15 min in a solution of **1** (9.8×10^{-4} M) and H_2O_2 (0.56 M), rinsed with PBS and used for the electrochemical detection with SECM.

3. Results and discussion

3.1. Localized immobilization of oligonucleotides onto thin gold films

The patterning of a thin gold film with oligonucleotides (ODN) was achieved through the local electrochemical deposition of polypyrrole-oligonucleotides (polypyrrole-ODN) using the direct mode of SECM, which constrains the current lines between the gold substrate and the microelectrode and allows localized electropolymerization (Fig. 1A).[3,17,20,43] The essence of this deposition method is based on the generation of high concentrations of pyrrole and pyrrole-ODN cation radical monomers in the gap between the gold substrate and the microelectrode (working in this case as a counter electrode) in order to locally deposit the conducting polymer. The requirement to form high concentrations of pyrrole and pyrrole-ODN radical cations is obtained by applying short potential pulses ($\tau = 20$ ms) to the gold substrate preventing the diffusion of the formed radical cations out into the solution. The choice of the potential at which the copolymerization takes place, but in particular the pulsing time as well as the distance between microelectrode and gold surface, are crucial for the formation of homogeneous pyrrole-ODN deposits. We have recently shown *via* fluorescence imaging,[17] that SECM does not, *a priori*, create a homogeneous distribution of polypyrrole/polypyrrole-ODN in the polypyrrole matrix. The pyrrole-ODN samples are concentrated at the outer dimension of the polymer spot due to the difference in the diffusion coefficients of pyrrole and pyrrole-ODN. The diffusion coefficient for pyrrole in aqueous solution is reported by Fulian and Compton to be $D_{pyrrole} = 1.25\ (\pm 0.1) \times 10^{-5}$ cm^2 s^{-1},[44]

while the diffusion coefficient of pyrrole-ODN is expected to be slightly lower due to the larger size of the molecule. These diffusion coefficients in addition to the slightly higher oxidation potential for pyrrole-ODN results in less efficient formation of pyrrole-ODN radical cations compared to pyrrole at the same potential. On the other hand, pyrrole-ODN, bearing several phosphate groups, is more soluble in aqueous solution compared to non substituted pyrrole such that the critical length for precipitation of the polymer is larger for pyrrole-ODN compared to unmodified pyrrole. As homogeneous spots are important for subsequent hybridization studies the distance between microelectrode and substrate was fixed in all our experiments at a distance of $z = 60$ μm. The optimal conditions for the local deposition of pyrrole-ODN films from a solution of pyrrole-ODN (10 μM) and pyrrole (200 mM) in $LiClO_4$ (0.1 M) were: (1) an oxidation potential of $E_{app} = 0.7$ V *vs.* Ag/AgCl, (2) a pulse time of $\tau = 20$ ms, (3) at a distance $z = 60$ μm.

3.2. Detection of the SECM deposited pyrrole-ODN spots

One of the key advantages of the direct mode of SECM is to produce localized micrometre size patterns similar to those fabricated by other microfabrication technologies.[29,45] SECM can be further used for the imaging of the formed polypyrrole microspots. This is however a real challenge as the thicknesses of the deposited spots are in the order of 20–50 nm.[20] Before using SECM as the method of detection, fluorescence imaging helped *a priori* to ensure the presence and homogeneity of the polypyrrole-ODN microspots[46] and to optimize the molecular assembly processes (Fig. 1C). Fig. 2 shows the fluorescence image of several polypyrrole-ODN microspots formed under different conditions ($E_{app} = 0.5$–2 V *vs.* Ag/Ag^+, $\tau = 10$ and 20 ms, $z = 60$ μm) after hybridization with its complementary biotinylated strand. The fluorescence labeling was achieved through a stepwise assembly with streptavidin and peroxidase-biotinamidocaproyl conjugate to which a fluorophore (5% streptavidin-*R*-phycoerythrin diluted in PBS) was linked. The fluorescence image shows that polypyrrole-ODN spots of about 100 μm were formed during the SECM "writing" process and that the assembly process (Fig. 1C) enables the detection of hybridization reactions on these ODN microspots. It furthermore shows that a potential of $E_{app} = 0.7$ V *vs.* Ag/Ag^+ for $\tau = 20$ ms (spots 2B, 2C, 2D) formed overall more homogeneous spots than at $E_{app} = 0.5$ V *vs.* Ag/Ag^+, and to some extent smaller spots than at higher potentials, and was thus used in the further experiments.

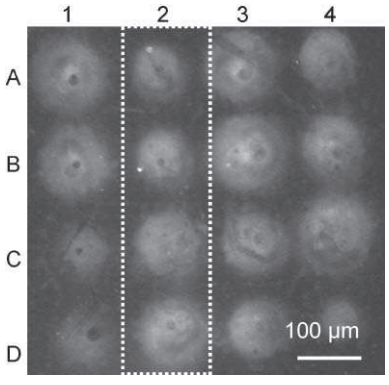

Fig. 2 Fluorescence image using an assembly approach of hybridized oligonucleotides formed *via* localized electropolymerization of pyrrole-ODN using SECM. Spotting conditions: $c_{pyrrole} = 200$ mM, $c_{pyrrole\text{-}ODN} = 10$ μM in $LiClO_4$ (0.1 M in water), $z = 60$ μm at different E_{app} and τ: **spots 1 (A, B, C, D)**: $E_{app} = 0.5$ V *vs.* Ag/Ag^+, $\tau = 20$ ms (A, B), $\tau = 10$ ms (C, D); **spots 2 (A, B, C, D)**: $E_{app} = 0.7$ V *vs.* Ag/Ag^+, $\tau = 10$ ms (A), $\tau = 20$ ms (B, C, D); **spots 3 (A, B, C, D)**: $E_{app} = 1.0$ V *vs.* Ag/Ag^+, $\tau = 20$ ms (A, B), $\tau = 10$ ms (C, D); **spots 4 (A, B, C, D)**: $E_{app} = 2.0$ V *vs.* Ag/Ag^+, $\tau = 10$ ms (A, B), $\tau = 20$ ms (C, D). Fluorescence imaging: exposure time = 0.32 s, fluorescence label: streptavidin-*R*-phycoerythrin. Hybridization conditions : $c_{complementary} = 0.1$ μM in hybridization buffer. Assembly conditions: streptavidin (0.5 mg mL^{-1}) for 30 min, HRP-biot (60 U mL^{-1}) for 45 min.

A key advantage of SECM in comparison to fluorescence imaging is that it allows visualization of the formed ODN microspots immediately after the electrochemical deposition without the use of a fluorescence labeling step and is thus an interesting alternative for the imaging of patterned surfaces. To image the polypyrrole-ODN microspots the feedback mode of SECM was used where by scanning the electrode over the surface and in the presence of a mediator, in our case $Ru(NH_3)_6^{3+}$, the steady state current on the microelectrode changed accordingly due to the alteration in local surface conductivity. As polypyrrole-ODN is a semiconductor a decreased positive feedback signal should be detected on the SECM tip compared to the surrounding high conducting gold surface. Fig. 3 shows the change in normalized current i_T/i (i is the measured current and i_T the current detected on the microelectrode in bulk solution) as a function of the distance z between the microelectrode and the gold surface in the vicinity of a polypyrrole-ODN microspot. Imaging of the polypyrrole-ODN spot is only possible for distances between $z = 5$–15 μm,

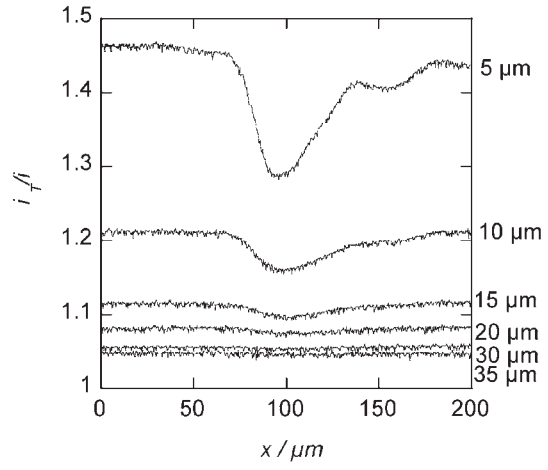

Fig. 3 Detection of pyrrole-ODN microspots using the feedback mode of SECM: influence of the scanning distance z between microelectrode and substrate. Scanning parameters: $Ru(NH_3)_6^{3+}$ (10mM) in KCl (0.1 M in water), scan rate: 20 μm s^{-1}, microelectrode (Pt, 10 μm diameter): E_{tip}: −0.5 V *vs.* Ag/Ag^+; substrate (gold modified with pyrrole-ODN spot) E_{sub} = open circuit potential. Spotting conditions: pyrrole-ODN (10 μM)–pyrrole (200 mM) in $LiClO_4$ (0.1 M in water); $\tau = 20$ ms; $E_{app} = 0.7$ V *vs.* Ag/Ag^+; $z = 60$ μm.

while at elevated distances the contrast between polypyrrole-ODN and the metallic support becomes negligible. The size of the spot is determined to be around 75 $\pm$ 5 μm which compares well with the fluorescence image in Fig. 2.

The influence of the scanning direction as well as of the scanning speed v on the polypyrrole-ODN images have also been investigated. Both parameters did not appear to alter the SECM image of the polypyrrole-ODN microspot giving confirmation that the microspots are not being distorted during scanning and are not influenced by the presence of the microelectrode. Scan rates as high as 100 μm s^{-1} could be used to acquire high resolution images allowing a relatively fast imaging of several ODN spots.

While SECM enables determination of the size of the formed ODN microspots, it is not capable of giving direct information about the thickness of the formed polymer film. Surface Plasmon Resonance (SPR), a surface-sensitive spectroscopic technique that can characterize ultra-thin organic films and multilayers on gold surfaces[47] was hence used. The surface selectivity of SPR arises from the enhancement of optical electrical fields at metal surfaces when surface plasmon polaritons are created at the metal/dielectric interface. Surface plasmon polaritons are excited on gold surfaces when p-polarized light illuminates the gold/dielectric interface through a prism under total reflection, coupling under a certain angle the incident light into surface plasmon modes. The formation of the plasmon is linked to a noticed decrease in the light reflectivity measured by the detector. The position of this minimum light reflectivity at the resonance angle is extremely sensitive to any changes in the index of refraction (n) of the adjacent medium and any change in the optical thickness. Fig. 4 shows the change of the intensity of the reflected light as a function of incident angle for the thin gold film and after polypyrrole-ODN has been deposited. SPR curves were fitted using the Winspall 2.01 program and

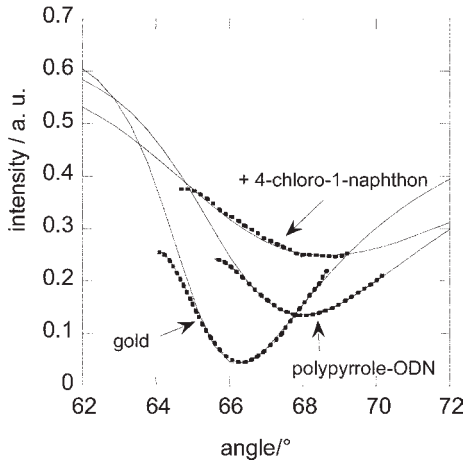

Fig. 4 Angular scan of the reflected intensity of the thin gold film and after the deposition of pyrrole-ODN. Dashed lines are experimental values, full lines correspond to fitted curves (n_{prism} = 1.58, $n_{titanium}$ = 2.36 + i3.11, d = 3 nm, n_{gold} = 0.287 + i3.4, d = 50 nm, $n_{solution}$ = 1.33, $n_{ppy–ODN}$ = 1.66 + i0.26 d = 5 nm, $n_{chloro\text{-}naphthon}$ = 1.396 + i0.08, d = 22 nm); spotting conditions: pyrrole-ODN (10 μM)–pyrrole (200 mM) in $LiClO_4$ (0.1 M in water); τ = 20 ms; E_{app} = 0.7 V *vs.* Ag/AgCl.

allowed determination of the film thickness of the deposited pyrrole film as well as of product (**2**). The following parameters were used for the fitting: $n_{titanium}$ = 2.36 + i3.11, n_{gold} = 0.287 + i3.4, n_{prism} = 1.58, $n_{ppy–ODN}$ = 1.7 + i0.3, $n_{chloro\text{-}naphthon}$ = 1.34 + i0.08. By fitting the experimental curves (dashed lines) to theoretical working curves (full line) the thickness of the polypyrrole-ODN films can be estimated. The determined film thicknesses for the polymer depended on the pulsing time.[17,20] For a pulsing time ofτ = 20 ms (which corresponds to the time of pulsing in the SECM experiments) polypyrrole-ODN film thicknesses between 1.5–8.0 nm were obtained.

As seen in Fig. 3, the change in conductivity caused by the presence of nanometer sized polymer films can be sensitively detected by the SECM tip, demonstrating the high potential of SECM as an imaging tool.

3.3. Detection of DNA hybridization using the feedback mode of SECM

To detect DNA hybridization we used once more the feedback mode rather than the generator-collection (GC) mode used by other groups where electroactive species generated by the immobilized biomolecule diffuse away from the surface and are detected by the SECM tip.[3,4] The feedback mode has been used so far mostly for the detection of immobilized enzymes[5,6,10,13] but is restricted to enzymes with high specific activity and high surface coverage. For the detection of the hybridization reaction on the polypyrrole-ODN microspots we take advantage of the formation of an insulating solid, 4-chloro-1-naphthon (**2**) which will block the regeneration of the mediator at the electrode surface (Fig. 1C). A change in the feedback current due to **2** is thus linked to successful ODN hybridization and molecular assembly. Fig. 1B shows the reaction scheme. The biotin tagged complementary (biotin-CP*) will react with streptavidin to which peroxidase-biotinamidocaproyl conjugate (HRP) will be linked. The HRP enzyme will in the presence of hydrogen peroxide (H_2O_2) stimulate the oxidation of 4-chloro-1-naphthol (**1**) to 4-chloro-1-naphthon (**2**),which is insoluble in the reaction medium and forms a precipitate only on the polypyrrole-ODN microspots, not on the unmodified gold surface.[39] Fig. 5 shows the change in normalized current as a function of distance d/a (a is the radius of the microelectrode and d is the measured distance) when the microelectrode is approaching the gold surface (Fig. 5A), with the polypyrrole-ODN modified surface (Fig. 5B) and after molecular assembly and biocatalytic oxidation of **1** in the presence of H_2O_2 using HRP (Fig. 5C). The kinetic fits according to Kwak and Bard[48] and Mirkin and Horrocks[49] are however of poor quality. Most of the kinetic information is in the short distance regime where no data points are available and it is thus not safe to deduce rate constants. However, qualitatively one can see that k_{eff} changes significantly for a gold surface, a surface modified with polypyrrole-ODN samples after molecular assembly and biocatalytic oxidation of **1** to **2**.

The SECM image of four electrochemical deposited polypyrrole-ODN samples after hybridization, assembly and biocatalytic oxidation of **1** to **2** is seen in Fig. 6B together

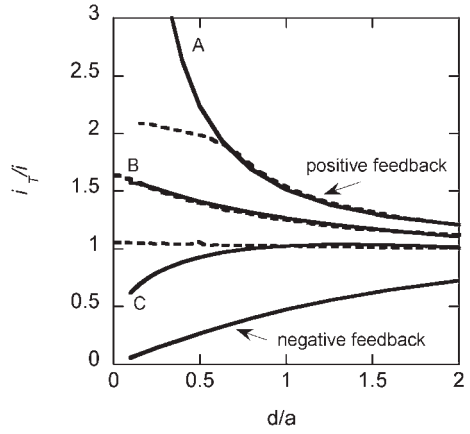

Fig. 5 Normalized current–distance curves recorded on diverse interfaces, theoretical curve (full line), experimental data (dotted lines) (**A**) pure gold surface, (**B**) gold surface covered with a pyrrole–oligonucleotide spot, spotting conditions: pyrrole–ODN (10 μM)–pyrrole (200 mM) in $LiClO_4$ (0.1 M in water); τ = 20 ms; E_{appl} = 0.7 V *vs.* Ag/Ag^+; z = 60 μm; (**C**) pyrrole–oligonucleotide covered gold surface after molecular assembly (streptavidin–HRP biotinylated, then incubation for 15 min in an aqueous solution of 4-chloro-1-naphthol (**1**, 9.8 × 10^{-4} M) and biocatalytic oxidation using H_2O_2 (0.56 M) for 15 min. Scanning parameters: $[Ru(NH_3)_6]^{3+}$ (10mM) in KCl (0.1 M in water), scan rate: 1 μm s^{-1}, microelectrode (Pt, 10 μm diameter): E_{tip}: −0.5 V *vs.* Ag/Ag^+; substrate (gold modified with pyrrole-ODN spot) E_{sub} = open circuit potential.

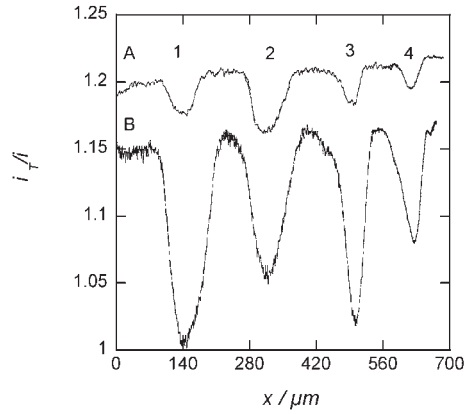

Fig. 6 Change of the detected feedback current over the current detected on the microelectrode by scanning over (**A**) an oligonucleotide spot and (**B**) over a hybridized oligonucleotide spot after biological assembly and formation of precipitate (**2**). Scanning parameters: $[Ru(NH_3)_6]^{3+}$ (10mM) in KCl (0.1 M in water), z = 10 μm, scan rate: 20 μm s^{-1}, microelectrode (Pt, 10 μm diameter): E_{tip}: −0.5 V *vs.* Ag/Ag^+; substrate (gold modified with pyrrole-ODN spot) E_{sub} = open circuit potential. Spotting conditions: pyrrole-ODN (10 μM)–pyrrole (200 mM) in $LiClO_4$ (0.1 M in water); τ = 20 ms; E_{appl} = 0.7 V *vs.* Ag/Ag^+; z = 60 μm; biological assembly: streptavidin–HRP biotinylated, then incubation for 15 min in an aqueous solution of 4-chloro-1-naphthol (**1**, 9.8 × 10^{-4} M).

with non hybridized polypyrrole-ODN microspots (Fig. 6A). The insulating precipitate (**2**) is formed with high precision around the deposited polypyrrole-ODN sample introducing only a slight increase in detected spot size. The apparent heterogeneous rate constant and thus the height of the

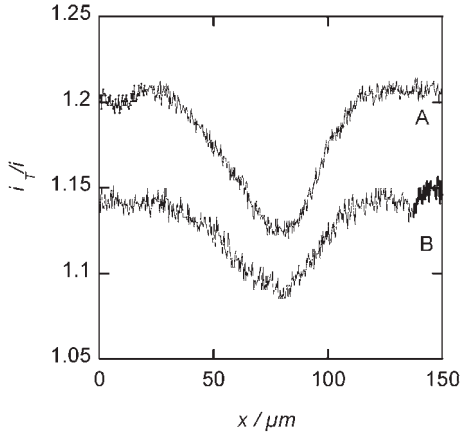

Fig. 7 Change of the detected feedback current during the biological assembly step, (**A**) current detected on the microelectrode by scanning over an oligonucleotide spot, (**B**) current detected on the microelectrode by scanning over a hybridized oligonucleotide spot modified with an assembly of streptavidin and biotinylated peroxidase. Scanning parameter: $[Ru(NH_3)_6]^{3+}$ (10mM) in KCl (0.1 M in water), z = 10 μm, scan rate: 20 μm s^{-1}, microelectrode (Pt, 10 μm diameter): E_{tip}: −0.5 V *vs.* Ag/Ag^+; substrate (gold modified with pyrrole-ODN spot) E_{sub} = open circuit potential. Spotting conditions: pyrrole-ODN (10 μM)–pyrrole (200 mM) in $LiClO_4$ (0.1M in water); τ = 20 ms; E_{appl} = 0.7 V *vs.* Ag/Ag^+; z = 60 μm.

normalized current changes slightly between the four spots but is distinctively different to the non hybridized case. However, the gold surface seems to have become less conducting as the i_T/i recorded on the hybridized microspots (Fig. 6B) is lower (1.15 instead of 1.21 recorded on the gold surface). That this partial blocking is due to the assembly process rather than the formed precipitate can be seen in Fig. 7. The normalized current in Fig. 7B, which corresponds to the assembly on the gold surface is of the same order as seen in Fig. 6B. It seems that the PBS–BSA used for the blocking of the gold surface to unspecific binding of biomolecules during hybridization is hindering the fast regeneration of the mediator. Additionally the assembly step also has a small influence on the SECM image of the polypyrrole-ODN microspots, where i_T/i is decreased. However, in comparison to the normalized current detected on the polypyrrole-ODN microspots where the biocatalytic oxidation of **1** to **2** had taken place a significant current reduction is observed. Indeed, as one can see from Fig. 4, by fitting the experimental SPR after molecular assembly and formation of **2**, a thickness of 22 ± 3 nm for the precipitate could be calculated for our conditions (n = 1.34 + i0.08). This makes the biocatalytic oxidation an interesting alternative to other hybridization detection methods.

The biocatalytic reaction in combination with SECM was furthermore used to investigate the ability to discriminate between complementary (biotin-CP*) and non complementary (biotin-M5*) ODN. Fig. 8 shows the change of the detected feedback currents recorded on the microelectrode for two polypyrrole-CP depositions (Fig. 8A) together with the feedback currents detected when polypyrrole-CP reacted with biotin-CP* (Fig. 8C) and biotin-M5* (Fig. 8B) and after the biocatalytic reaction had taken place (compare Fig. 6). Fig. 8

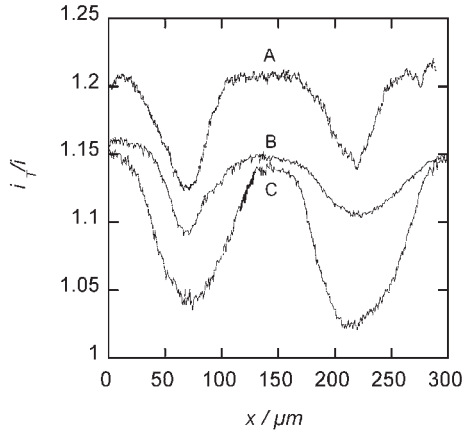

Fig. 8 Discrimination using complimentary and non complimentary hybridization targets. (**A**) Feedback currents over polypyrrole-CP spot. (**B**) Feedback currents after hybridization with biotin-M5* and biological assembly. (**C**) Feedback currents after hybridization with biotin-CP* and biological assembly. Scanning parameters: $[Ru(NH_3)_6]^{3+}$ (10 mM) in KCl (0.1 M in water), z = 10 μm, scan rate: 20 μm s^{-1}, microelectrode (Pt, 10 μm diameter): E_{tip}: −0.5 V *vs.* Ag/AgCl; substrate (gold modified with pyrrole-ODN spot) E_{sub} = open circuit potential. Spotting conditions: pyrrole-ODN (10 μM)–pyrrole (200 mM) in $LiClO_4$ (0.1 M in water); τ = 20 ms; E_{appl} = 0.7 V *vs.* Ag/AgCl; z = 60 μm. Biological assembly: streptavidin–HRP biotinylated, then incubation for 15 min in an aqueous solution of 4-chloro-1-naphthol (**1**, 9.8 × 10^{-4} M).

demonstrates that the SECM detection scheme can discriminate between complementary and non complementary hybridization targets. While a minor decrease in i_T/i was observed for the reaction with biotin-M5*, the change in i_T/i using biotin-CP* targets was significant. Furthermore, this experiment shows that subsequent hybridization/denaturation is possible without the destruction of the polymer film. Indeed, between these two hybridization and biocatalytic experiments, the surface had to be regenerated. This was possible by rinsing the assembly first with 1% SDS in PBS and then with 200 mM NaOH to dehybridize the DNA.

4. Conclusion

The successful combination of using SECM imaging for localized DNA hybridization on a DNA microarray formed *via* SECM microspotting has been demonstrated. The hybridization method relies on the inherent sensitivity of SECM to the detection of the small variations of surface conductivity initiated by the local deposition of an insulating solid, 4-chloro-1-naphthon (**2**). This product was formed through the biocatalysis of 4-chloro-1-naphthol (**1**) in the presence of hydrogen peroxide by HRP, which has been linked through molecular assembly using streptavidin/biotin chemistry to hybridized ODN probes. That the presence of nanometre sized films can be sensitively detected by the SECM tip demonstrates the high potential of SECM as an imaging tool. The method was found to be highly reproducible, fast and easy to perform and thus shows its importance for the use of DNA chips. Hybridization and dehybridization is possible without the destruction of the polymer layer. The method showed a good discrimination between complementary and non complementary ODN targets.

Acknowledgements

The gold deposition was performed at the platform PROMESS at the DRFMC of the CEA Grenoble.

References

1 Y. Xia and G. M. Whitesides, *Angew. Chem., Int. Ed.*, 1998, **37**, 550.
2 E. Delamarche, A. Bernard, H. Schmidt, A. Bietsche, B. Michel and H. Biebuyck, *J. Am. Chem. Soc.*, 1998, **120**, 500.
3 S. A. G. Evans, C. Brakha, M. Billon, P. Mailley and G. Denuault, *Electrochem. Commun.*, 2005, **7**, 135–140.
4 R. E. Gyurcsanyi, G. Jagerszki, G. Kiss and K. Toth, *Bioelectrochemistry*, 2004, **63**, 207–215.
5 C. Kranz, G. Wittstock, H. Wohlschlager and W. Schuhmann, *Electrochim. Acta*, 1997, **42**, 3105–3111.
6 M. Niculescu, S. Gaspar, A. Schulte, E. Csoregi and W. Schuhmann, *Biosens. Bioelectron.*, 2004, **19**, 1175–1184.
7 F. Turcu, A. Schulte, G. Hartwich and W. Schuhmann, *Biosens. Bioelectron.*, 2004, **20**, 5, 925–932.
8 J. Wang, F. Song and F. Zhou, *Langmuir*, 2002, **18**, 6653–6658.
9 J. Wang and F. Zhou, *J. Electroanal. Chem.*, 2002, **537**, 95.
10 C. A. Wijayawardhana, G. Wittstock, H. B. Halsall and W. R. Heinemann, *Anal. Chem.*, 2000, **72**, 333–338.
11 T. Wilhelm and G. Wittstock, *Langmuir*, 2002, **18**, 9485–9493.
12 C. Zhao and G. Wittstock, *Biosens. Bioelectron.*, 2005, **20**, 1277–1284.
13 J. Zhou, C. T. Campbell, A. Heller and A. J. Bard, *Anal. Chem.*, 2002, **74**, 4007–4010.
14 T. Wilhelm and G. Wittstock, *Electrochim. Acta*, 2001, **47**, 275–281.
15 G. Wittstock and W. Schuhmann, *Anal. Chem.*, 1997, **69**, 5059.
16 I. Turyan, T. Matsue and D. Mandler, *Anal. Chem.*, 2000, **72**, 3431.
17 E. Fortin, Y. Defontaine, P. Mailley, T. Livache and S. Szunerits, *Electroanalysis*, 2005, **17**, 495–503.
18 C. Kranz, M. Ludwig, H. E. Gaub and W. Schuhmann, *Adv. Mater.*, 1995, **7**, 38.
19 C. Kranz, M. Ludwig, H. E. Gaub and W. Schuhmann, *Adv. Mater.*, 1995, **7**, 568–571.
20 S. Szunerits, N. Knorr, R. Calemczuk and T. Livache, *Langmuir*, 2004, **20**, 9236–9241.
21 W. B. Nowall, W. B. Wipf and W. G. Kuhr, *Anal. Chem.*, 1998, **70**, 2601–2606.
22 H. Shiku, T. Takeda, H. Yamada and T. Matsue, *Anal. Chem.*, 1995, **69**, 5059.
23 B. Liu, S. A. Rotenber and M. V. Mirkin, *Proc. Natl. Acad. Sci. USA*, 2000, **97**, 9855.
24 K. Yamashita, M. Takagi, K. Uchida, H. Kondo and S. Takenaka, *Analyst*, 2001, **126**, 1210.
25 E. Paleek, *Talanta*, 2002, **56**, 809–819.
26 J. Wang, *Anal. Chim. Acta*, 2002, **469**, 63–71.
27 P. Guedon, T. Livache, F. Martin, F. Lesbre, A. Roget, G. Bidan and Y. Levy, *Anal. Chem.*, 2000, **72**, 6003.
28 N. Lassalle, P. Mailley, E. Viel, T. Livache, A. Roget, J. P. Correia and L. M. Abrantes, *J. Electroanal. Chem.*, 2001, **509**, 48.
29 T. Livache, H. Bazin, P. Caillat and A. Roget, *Biosens. Bioelectron.*, 1998, **13**, 629.
30 T. Livache, B. Fouque, A. Roget, J. Marchand, G. Bidan, R. Teoule and G. Mathis, *Anal. Biochem.*, 1998, **255**, 188.
31 T. Livache, P. Guedon, C. Brakha, A. Roget, Y. Levy and G. Bidan, *Synth. Met.*, 2001, **121**, 1443–1444.
32 T. Livache, A. Roget, E. Dejean, C. Barthet, G. Bidan and R. Teoule, *Nucleic Acids Res.*, 1994, **22**, 2915–2921.
33 T. Livache, A. Roget, E. Dejean, C. Barthet, G. Bidan and R. Teoule, *Synth. Met.*, 1995, **71**, 2143–2146.
34 S. Cosnier, *Biosens. Bioelectron.*, 1999, **14**, 443–456.
35 A. I. Minett, J. N. Barisci and G. G. Wallace, *Anal. Chim. Acta*, 2003, **475**, 37–45.

36 S. Serradilla Razola, B. Lopez Ruiz, N Mora Diez, H. B. Mark and J.-M. Kauffmann, *Biosens. Bioelectron.*, 2002, **17**, 921–928.
37 J.-C. Vidal, J. Espuelas, E. Garcia-Ruiz and J.-R. Castillo, *Talanta*, 2004, **64**, 655–664.
38 J. Wang, N. V. Myung, M. Yun and H. G. Monbouquette, *J. Electroanal. Chem.*, 2005, **575**, 139–146.
39 L. Alfonta, A. K. Singh and I. Willner, *Anal. Chem.*, 2001, **73**, 91.
40 K. Borgwarth, D. Ebling and J. Heinze, *Electrochim. Acta*, 1995, **40**, 1455.
41 T. Wink, S. J. Van Zuilen, A. Bult and W. P. van Bennekom, *Anal. Chem.*, 1998, **70**, 827–832.
42 R. P. H. Kooyman, A. T. M. Lenferink, R. G. Eenink and J. Greve, *Anal. Chem.*, 1991, **63**, 83–85.
43 S. Szunerits, L. Bouffier, R. Calemczuk, B. Corso, M. Demeunynck, E. Descamps, Y. Defontaine, J.-B. Fiche, E. Fortin, T. Livache, P Mailley, A. Roget and E. Vieil, *Electroanalysis*, 2005 in press.
44 Q. Fulian and R. G. Compton, *Anal. Chem.*, 2000, **72**, 1830.
45 R. Georgiadis, K. A. Peterlinz, J. R. Rahn, A. W. Peterson and J. H. Grassi, *Langmuir*, 2000, **16**, 6759–6762.
46 A. Depont-Filliard, A. Roget, T. Livache and M. Billon, *Anal. Chim. Acta*, 2001, **449**, 45.
47 A. G. Frutos and R. M. Corns, *Anal. Chem*, 1998, **70**, 449A.
48 J. Kwak and A. J. Bard, *Anal. Chem.*, 1989, **61**, 1221.
49 M. V. Mirkin and B. R. Horrocks, *Anal. Chim. Acta*, 2000, **406**, 119.